Supplemental Material
Optics formula and additional results

1 Fresnel equations

We reproduce the Fresnel equations derived from Maxwell equations as given by Born and Wolf (Section 14.4.1). They correspond to the configuration of a dielectric layer of real index η_a over a conducting layer of complex index $\eta_b + i\kappa_b$. In our model, we use them both for the thin-film/base interface (i.e., with $a = 2$ and $b = 3$) and the air/thin-film interface (i.e., with $a = 1$, $b = 2$ and $\kappa_b = \kappa_2 = 0$). Born and Wolf use a slightly different notation for the complex index: $\eta_b(1 + ik_b)$ (hence $\kappa_b = \eta_b k_b$). We adapt their equations to conform to our notations. The complex reflection coefficient depends on the angle of incidence θ_a and is written $\mathbf{r}_{ab} = r_{ab}e^{i\phi_{ab}}$, with:

$$\begin{aligned} |r_{ab}^{\perp}|^2 &= \frac{(\eta_a \cos\theta_a - u_b)^2 + v_b^2}{(\eta_a \cos\theta_a + u_b)^2 + v_b^2} \\ \tan(\phi_{ab}^{\perp}) &= \frac{2v_b\eta_a \cos\theta_a}{u_b^2 + v_b^2 - \eta_a^2 \cos^2\theta_a} \end{aligned}$$

for polarization perpendicular to the incidence plane; and

$$\begin{aligned} |r_{ab}^{\parallel}|^2 &= \frac{[(\eta_b^2 - \kappa_b^2)\cos\theta_a - \eta_a u_b]^2 + [2\eta_b\kappa_b \cos\theta_a - \eta_a v_b]^2}{[(\eta_b^2 - \kappa_b^2)\cos\theta_a + \eta_a u_b]^2 + [2\eta_b\kappa_b \cos\theta_a + \eta_a v_b]^2} \\ \tan(\phi_{ab}^{\parallel}) &= 2\eta_a \cos\theta_a \frac{2\eta_b\kappa_b u_b - (\eta_b^2 - \kappa_b^2)v_b}{(\eta_b^2 + \kappa_b^2)^2 \cos^2\theta_a - \eta_a^2(u_b^2 + v_b^2)} \end{aligned}$$

for polarization parallel to the incidence plane, where

$$\begin{array}{l} u_b = \frac{\sqrt{U+V}}{2} \\ v_b = \frac{\sqrt{V-U}}{2} \end{array} \quad \text{with} \quad \left\{ \begin{array}{l} U = \eta_b^2 - \kappa_b^2 - \eta_a^2 \sin^2\theta_a, \\ V = \sqrt{U^2 - 4\kappa_b^2}. \end{array} \right.$$

The amplitude coefficients $r_{ab}^{\perp}$ and $r_{ab}^{\parallel}$ are visualized in red and green colors respectively in Figure 1(a). Each curve corresponds to a different value of κ_b, which is related to the conductivity of the base material. The darker the color, the lower the value of κ_b, with the darkest curves corresponding to $\kappa_b = 0$ (i.e., a dielectric base layer). The phase shifts $\phi_{ab}^{\perp}$ and $\phi_{ab}^{\parallel}$ are visualized with the same color convention in Figure 1(b). For a dielectric base (darkest curves), $\phi_{ab}^{\perp}$ equals 0 for all elevation angles, whereas $\phi_{ab}^{\parallel}$ suddenly jumps from 0 to π at the so-called Brewster's angle. This does not actually correspond to a discontinuity in complex reflectances, since at this same angle, $r_{ab}^{\parallel} = 0$ as seen in Figure 1(a). This is better visualized in Figure 1(c), which shows the complex reflectance coefficient $\mathbf{r}_{ab}$ in the complex plane. When $\kappa_b \to 0$ (darker colors), $\mathbf{r}_{ab}$ tends toward the real axis. In the limit where $\kappa_b = 0$, $\mathbf{r}_{ab}^{\perp}$ (in red) remains on the positive side of the real axis, but $\mathbf{r}_{ab}^{\parallel}$ (in green) changes sign, which is accounted by the phase shift of π. The blue curve corresponds to the complex reflection coefficient at normal incidence (i.e., $\theta_a = 0$), where we have:

$$\begin{aligned} |r_{ab}^{\perp}|^2 = |r_{ab}^{\parallel}|^2 &= \frac{(\eta_a - \eta_b)^2 + \kappa_b^2}{(\eta_a + \eta_b)^2 + \kappa_b^2}, \\ \tan(\phi_{ab}^{\perp}) = \tan(\phi_{ab}^{\parallel}) &= \frac{2\eta_a\kappa_b}{\eta_b^2 + \kappa_b^2 - \eta_a^2}. \end{aligned}$$

This is also visible in Figure 1(a,b) where curves for a same κ_b but different polarizations start with the same value at $\theta_a = 0$. Ovserve that at $\theta_a = \pi/2$ and irrespective of the value of κ_b, the amplitude coefficients for both polarizations end up being equal to 1, whereas the phases differ by an angle of π between polarizations; hence $\mathbf{r}_{ab}^{\perp} = 1$ and $\mathbf{r}_{ab}^{\parallel} = -1$, as seen in Figure 1(c).

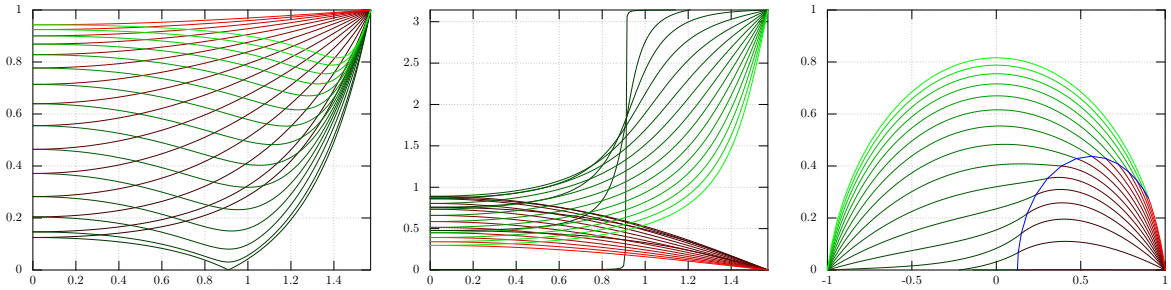

(a) Amplitudes $|r_{ab}|$ (b) Phases ϕ_{ab} (c) Complex coefficients $\mathbf{r}_{ab}$

Figure 1: Visualization of Fresnel coefficients for perpendicular and parallel polarizations (in red and green respectively) as a function of the incident angle θ_a. We use a dielectric layer of constant index $\eta_a = 1.4$ over a conducting layer of constant index $\eta_b = 1.8$, with a varying $\kappa_b \in \{0.0, 0.138, 0.293, 0.469, 0.667, 0.897, 1.156, 1.450, 1.785, 2.165, 2.597, 3.088, 3.645, 4.279, 5.0\}$ shown with curves of different intensities (the darker the curve, the lower κ_b). In (a) we show the amplitude of the Fresnel coefficients, which appears seemingly discontinuous for the parallel component when $\kappa_b = 0$, at Brewster's angle. As shown in (b), the corresponding phase is also discontinous, suddenly switching from 0 to π. There is no actual discontinuity as shown in (c): when $\kappa_b = 0$, the curve lies on the real axis and crosses 0 at Brewster's angle for the parallel component. The complex reflection coefficients at incidence are shown by the blue curve in (c).

Our method rely on computing separately the response to parallel and perpendicular polarizations. We motivate this with Figure 2 where a real-life example is shown. The two orthogonal polarizations have a different color pattern. Since the Fresnel coefficients are used nonlinearly in Airy's summation, we cannot use the average Fresnel coefficient and phase to compute the average color pattern.

Unpolarized Close-up polarized Close-up orthogonal polarization

Figure 2: Polarization impacts iridescent colors. In this real example, we photographed a thin-film material with a polarization filter. Comparing one polarization to its orthogonal polarization, we observe changes in the color patterns. This example illustrates the need to compute both parallel and perpendicular polarizations separately to obtain the correct average color fringe pattern.

2 Optical path difference

The optical path difference (OPD) on reflection is classically computed by comparing a ray reflected at the first interface, with a ray reflected once at the second interface. This is shown in Figure 3(a). The OPD between the first and second rays (i.e., at order $k = 1$) is then given by $\mathcal{D} = \eta_2(AB + BC) - \eta_1 AD$, where the refractive indices account for the difference of wavelength in different media. Since $AB = BC = d/\cos(\theta_2)$, and $\eta_1 AD = 2d\tan(\theta_2)\eta_1 \sin(\theta_1) = 2d\tan(\theta_2)\eta_2 \sin(\theta_2)$ according to Snell's law, we obtain $\mathcal{D} = 2\eta_2 d\cos\theta_2$ after a few simplifications. At order k, the primary ray is compared to a ray reflected k times at the second interface, hence exiting at a distance kAD from the incident location. Hence the optical difference becomes $\mathcal{D}(k) = \eta_2 k(AB + BC) - \eta_1 kAD$, yielding $\mathcal{D}(k) = k\,\mathcal{D}$.

The optical path difference (OPD) on transmission is computed by comparing a ray transmitted through both interfaces, with a ray undergoing two additional reflections, one at each interface. This is shown in Figure 3(b). The OPD is now given by $\mathcal{D} = \eta_2(AB + BC) - \eta_3 AD$. Interestingly, since $\eta_3 AD = 2d\tan(\theta_2)\eta_3 \sin(\theta_3) = 2d\tan(\theta_2)\eta_2 \sin(\theta_2)$ according to Snell's law as before, the OPD on transmission is actually identical to the OPD on reflection.

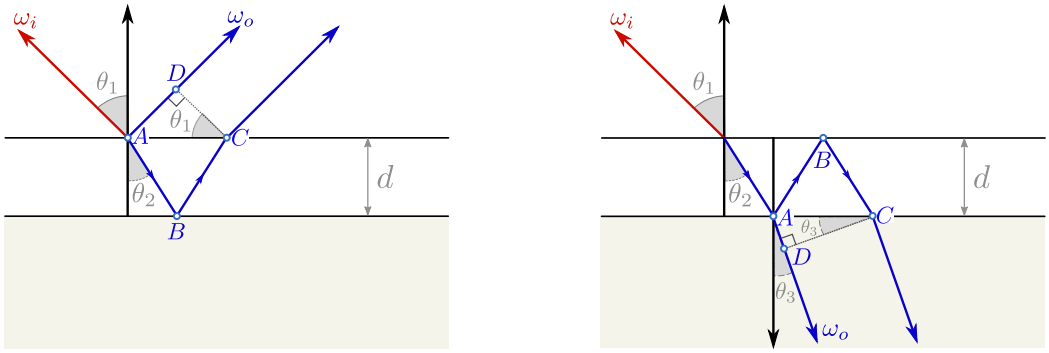

(a) OPD on reflection (b) OPD on transmission

Figure 3: The OPD on reflection (a) and transmission (b) are derived by comparing directly reflected/transmitted rays to rays that undergo additional reflections in the thin-film layer.

3 Varying-index datasets

Here, we show three examples of dielectric thin-films applied over a dieletric or conducting base, with both layers having refractive indices that vary with wavelength. In two examples (Glass and Silver bases covered by a film of Butanol, first and second column respectively), the pre-integrated reflectance model closely matches the chromatic curve of the ground truth. Observe that in both cases, the real part of IOR is constant while the complex part is monotonous (as shown in the first line). In the third column, where we use copper for the base material, the pre-integrated reflectance shows more difference with the reference. This is probably due to the variation in IOR of the base material with respect to each sentivity curve. These differences would likely be reduced if more spectral bands where available.

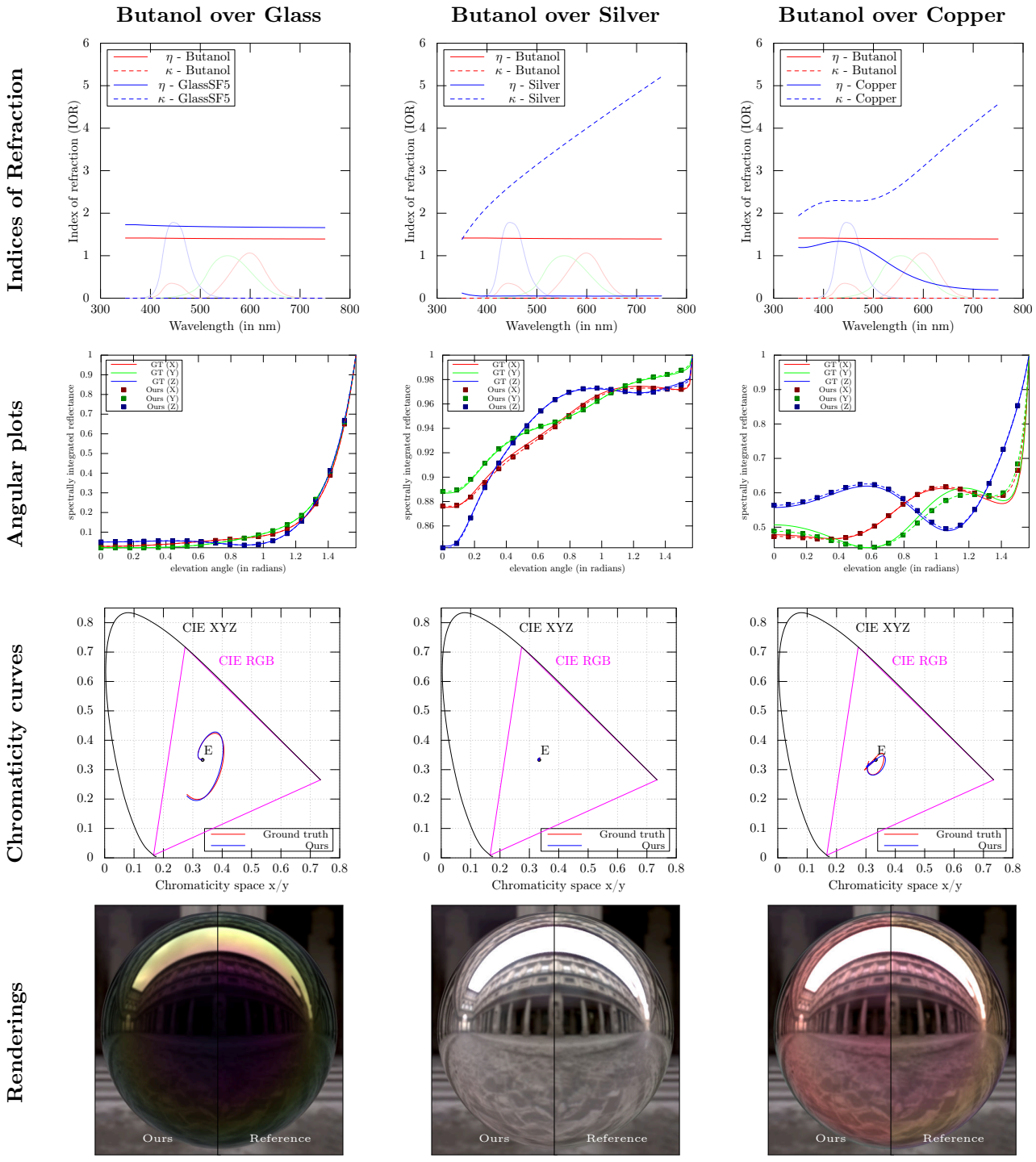

4 Comparison with Ergun et al.

We have reproduced below the results of Ergun et al. (their Figure 7) by adjusting the parameters of our model by hand. Each vertical pair of images shows Ergun et al.'s approach on top and ours below. Our method permits to produce very similar color fringes with a much simpler model. The remaining differences mostly concern in color saturation. This which might be due to multi-layered thin-film intereference effects, which we do not model. The parameters used for our model are detailed in the table below (we set $\alpha = 0.07$ throughout):

$\mathcal{D}_{inc} = 91$ nm $\eta_2 = 3.0$ $\eta_3 = 1.43$ $\kappa_3 = 0.0$	$\mathcal{D}_{inc} = 570$ nm $\eta_2 = 1.8$ $\eta_3 = 1.08$ $\kappa_3 = 0.51$	$\mathcal{D}_{inc} = 620$ nm $\eta_2 = 3.0$ $\eta_3 = 1.49$ $\kappa_3 = 0.95$	$\mathcal{D}_{inc} = 620$ nm $\eta_2 = 2.83$ $\eta_3 = 1.19$ $\kappa_3 = 0.72$
$\mathcal{D}_{inc} = 665$ nm $\eta_2 = 1.97$ $\eta_3 = 1.12$ $\kappa_3 = 0.0$	$\mathcal{D}_{inc} = 1020$ nm $\eta_2 = 1.79$ $\eta_3 = 1.79$ $\kappa_3 = 0.0$	$\mathcal{D}_{inc} = 1110$ nm $\eta_2 = 1.77$ $\eta_3 = 1.77$ $\kappa_3 = 0.09$	$\mathcal{D}_{inc} = 1140$ nm $\eta_2 = 1.97$ $\eta_3 = 1.97$ $\kappa_3 = 0.1$

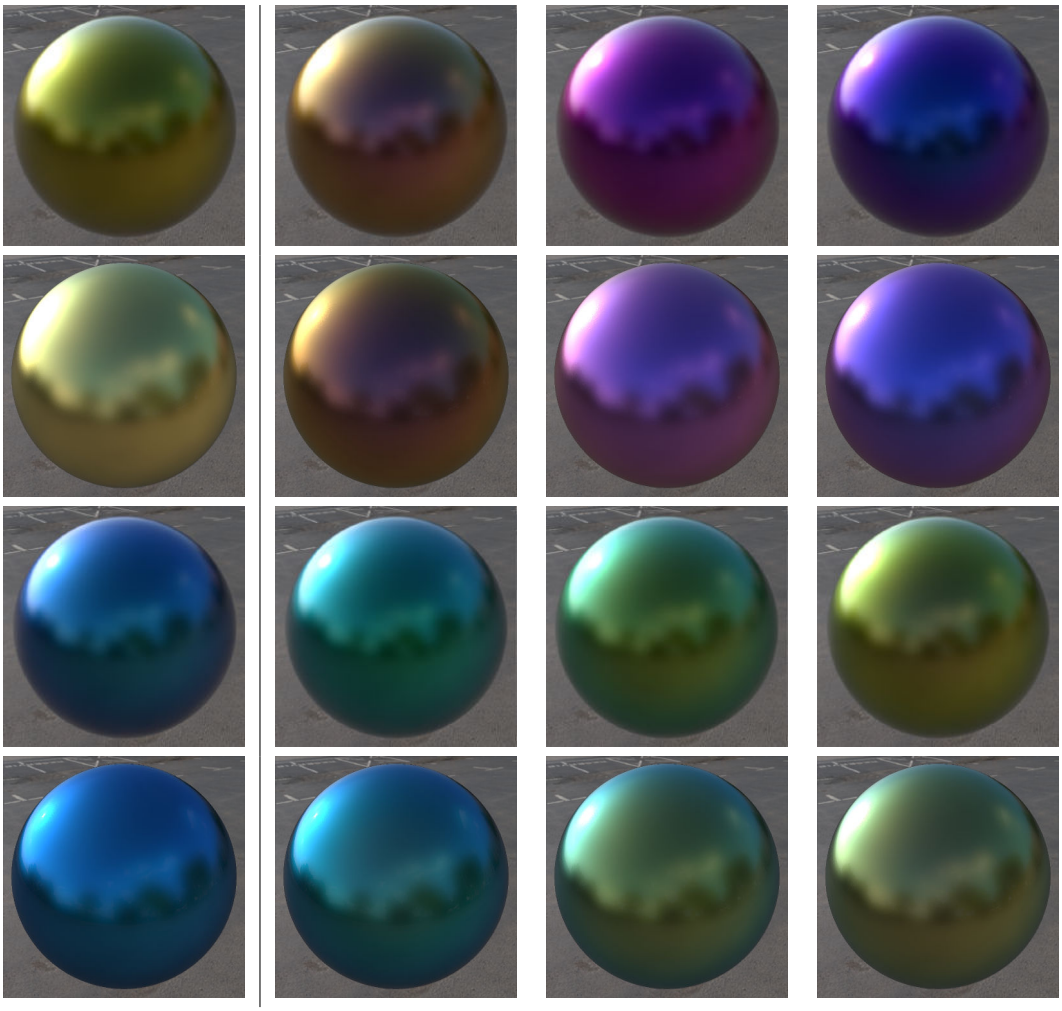

5 Appearance Range

Here we display some achievable appearances for a thin-film with a constant index of refraction $\eta_2 = 1.33$, a thickness in the range $[300..800]$nm and a base with an index of refraction in $\{1, 1.28, 1.38, 1.85, 2.71\}$.

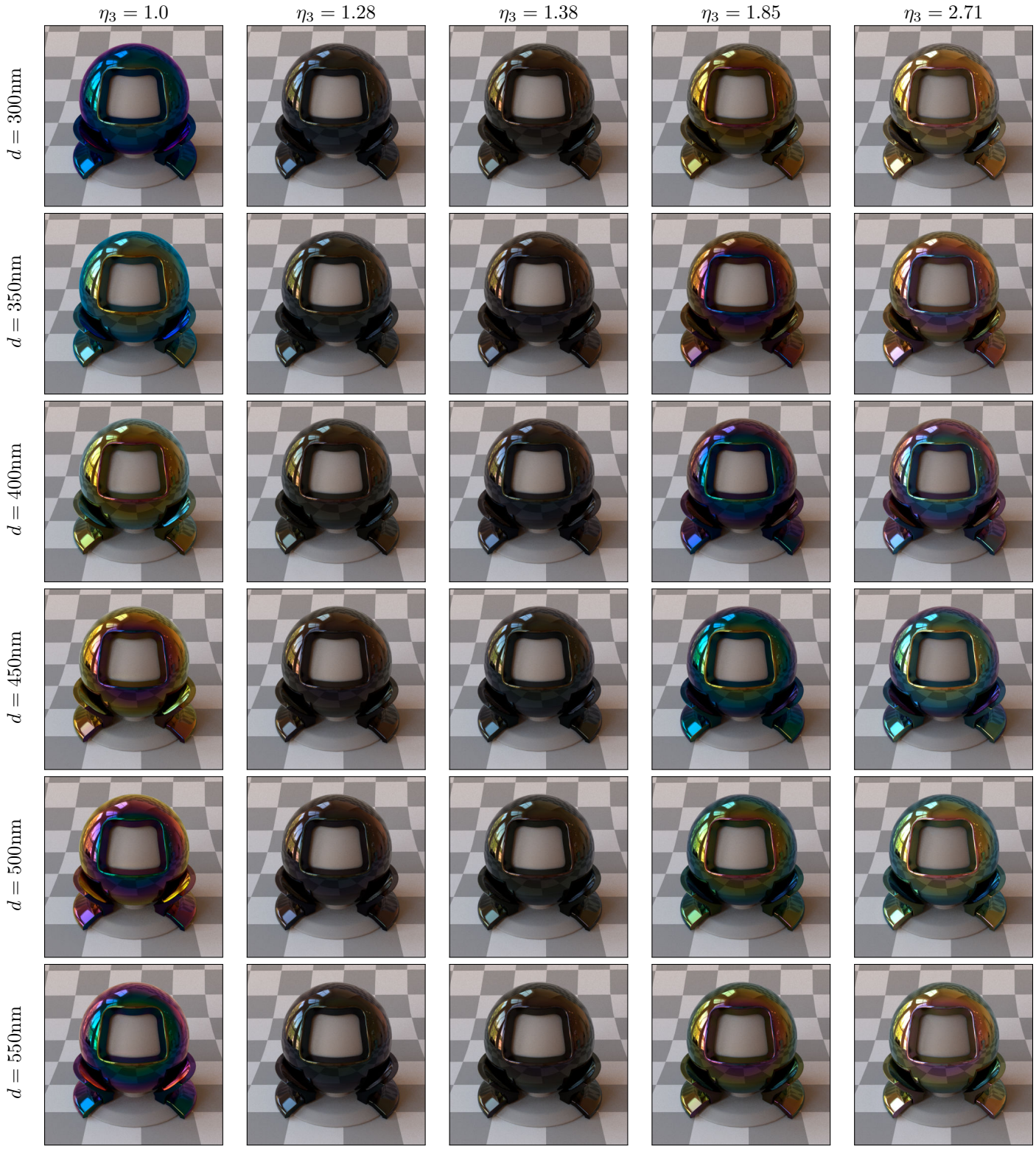

We can see that, for a constant thickness d, we obtain very different appearances for $\eta_2 > \eta_3$ and $\eta_2 < \eta_3$ but not for different values of η_3 when $\eta_2 < \eta_3$. For η_3 close to η_2 we see a darkening of colors as the reflectance $R23$ goes to one. However note that the reflectance still contains a subtle chromatic effect that can be used to get effects such as leather coating.

We also give results for a conducting base with $\kappa_3 \in \{0.0, 0.5, 1.0, 1.5, 2.0\}$.

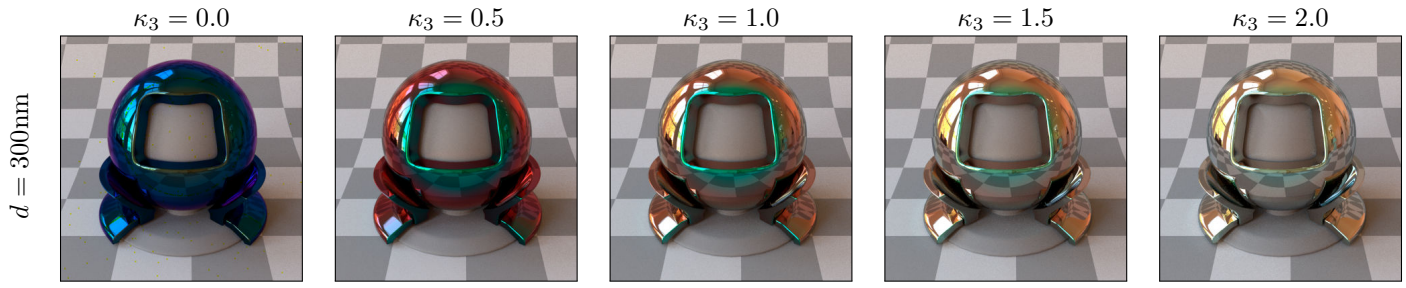


$\kappa_3 = 0.0$
$\kappa_3 = 0.5$
$\kappa_3 = 1.0$
$\kappa_3 = 1.5$
$\kappa_3 = 2.0$
$d = 350$nm
$d = 400$nm
$d = 450$nm
$d = 500$nm
$d = 550$nm
$d = 600$nm

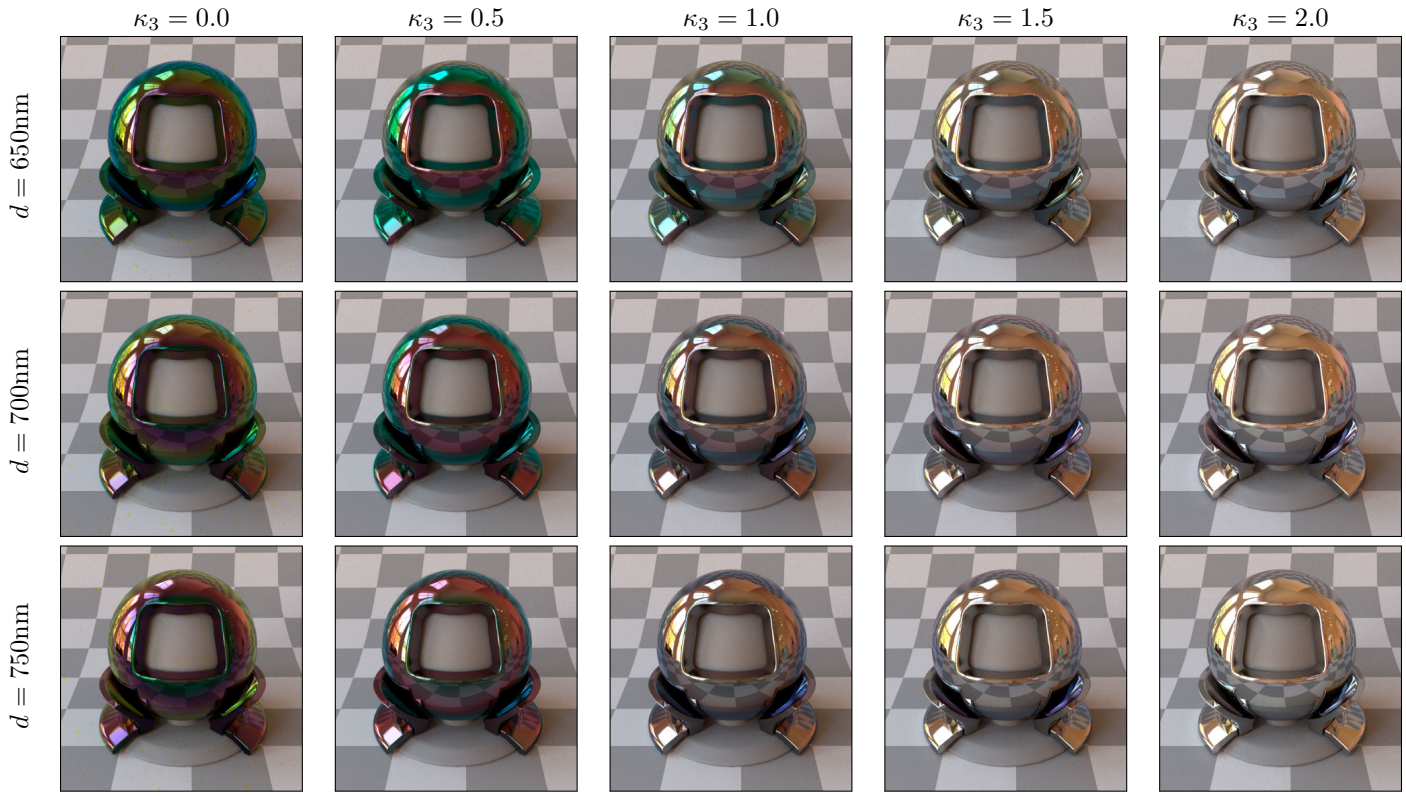
$\kappa_3 = 0.0$
$\kappa_3 = 0.5$
$\kappa_3 = 1.0$
$\kappa_3 = 1.5$
$\kappa_3 = 2.0$
$d = 650\text{nm}$
$d = 700\text{nm}$
$d = 750\text{nm}$

6 Steel tempering

We reproduce the appearance of tempered steel (an iron alloy) for different tempering temperatures. In the following image (found on Wikipedia), different plates of the same steel have been tempered for an hour at different temperatures (350°F to 730°F). The metallic parts have been roughned for the photograph.

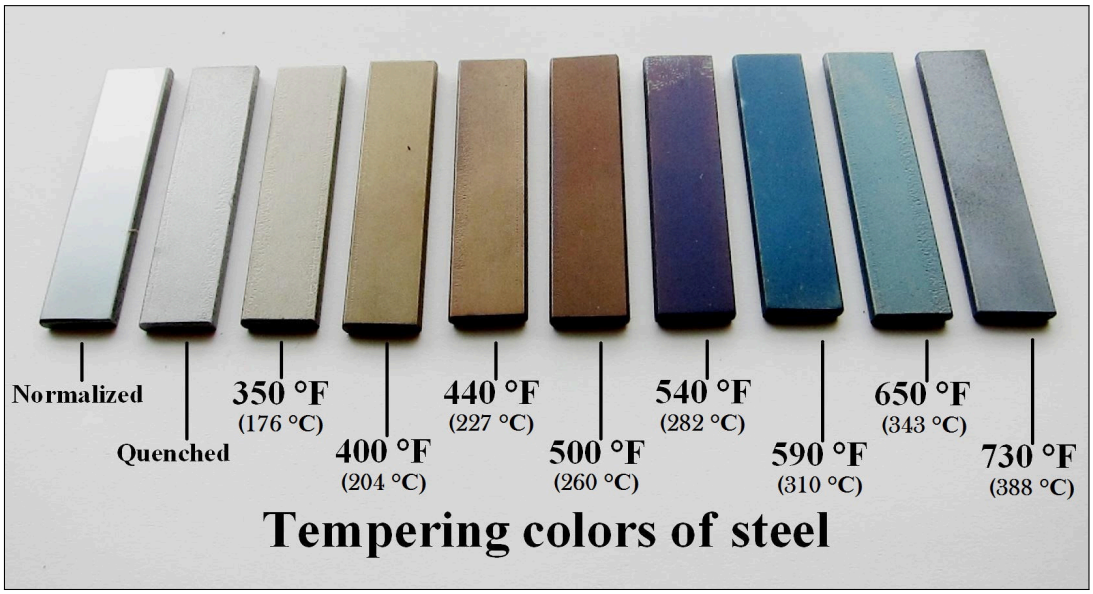

Source: https://en.wikipedia.org/wiki/Tempering_(metallurgy)

We reproduce the picture setup using a large rectangular light, and different steel rectangles using the index of refraction of iron (roughly $\eta = 2.7$, $\kappa = 2.8$) and $\eta = 2.9$ for the index of refraction of the oxide for all the bars[1]. As the thickness of the oxide increases with temperature, we monotonically increase the thickness parameter from $d = 10$nm (second from the left) to $d = 70$nm (right most).

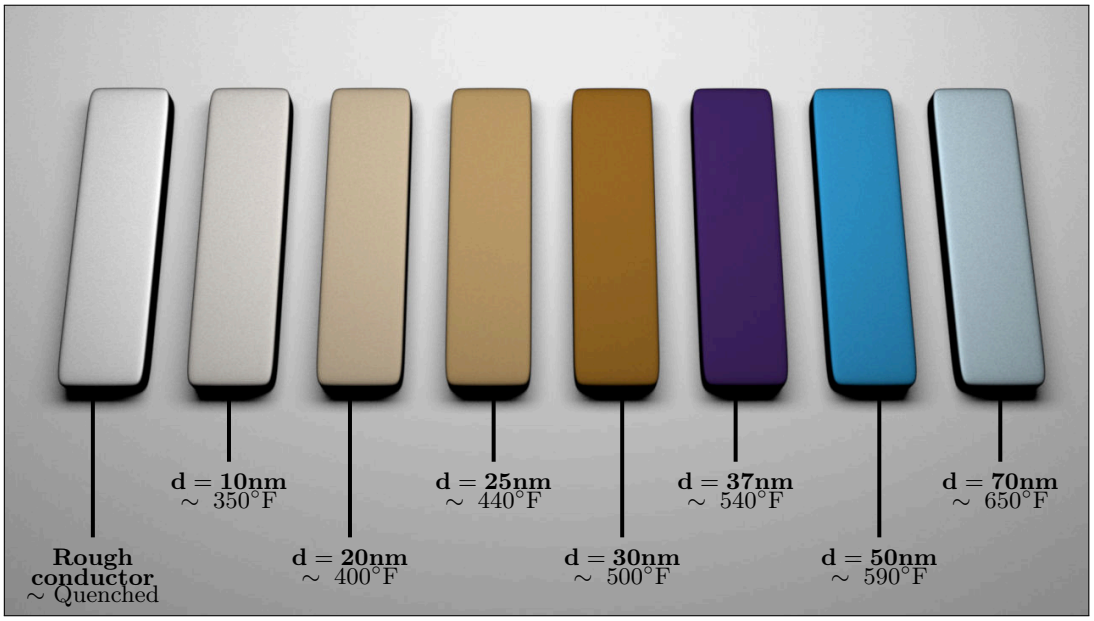

[1] We have found those IORs on http://refractiveindex.info/?shelf=main&book=Fe&page=Werner and http://www.filmetrics.com/refractive-index-database/Fe2O3/Iron-Oxide